

# Polarographic and Spectrophotometric Investigation of Iron(III) Complexation to 3,4-Dihydroxyphenylalanine-Containing Peptides and Proteins from *Mytilus edulis*

Steven W. Taylor,\* George W. Luther III, and J. Herbert Waite

College of Marine Studies and Department of Chemistry and Biochemistry, University of Delaware, Newark, Delaware 19716

Received February 3, 1994<sup>⊗</sup>

The iron(III) binding properties of *Mytilus edulis* foot protein 1 (Mefp1), its component peptides hexapeptide A (A<sub>1</sub>K<sub>2</sub>P<sub>3</sub>T<sub>4</sub>Y<sub>5</sub>K<sub>6</sub>; Y<sub>5</sub> = 3,4-dihydroxyphenylalanine (DOPA)) and decapeptides B to E (A<sub>1</sub>K<sub>2</sub>P<sub>3</sub>S<sub>4</sub>Y<sub>5</sub>P<sub>6</sub>P<sub>7</sub>T<sub>8</sub>Y<sub>9</sub>K<sub>10</sub>; peptides B to E: P<sub>6</sub> = 3-hydroxyproline (3HYP), P<sub>7</sub> = 4HYP, Y<sub>9</sub> = DOPA; peptide B: P<sub>3</sub> = 4HYP, Y<sub>5</sub> = DOPA; peptide C: P<sub>3</sub> = 4HYP; peptide D: Y<sub>5</sub> = DOPA), and their synthetic decapeptide analogues (peptide S<sub>1</sub>: Y<sub>9</sub> = DOPA; peptide S<sub>2</sub>: Y<sub>5</sub> = Y<sub>9</sub> = DOPA) have been investigated by polarography and spectrophotometry. A "chelate scale" was constructed by measuring the reduction potentials of iron(III) complexes with known stability constants and was used to estimate stability constants for the iron(III) interactions with peptides. A linear relationship was found to exist between the reduction potentials and the pH independent thermodynamic stability constants for iron(III) complexes spanning 20 orders of magnitude in chelate stability. Spectrophotometric data allowed the stoichiometry of the peptide–iron(III) interactions to be determined. At neutral pH all peptides favored an intermolecular bis(catecholato) coordination mode, through the DOPA nearest the C terminus. Reasons for the extra stability observed in the peptide complexes compared with simple catecholates are offered, with the possibility of hydroxyproline involvement eliminated on the basis of comparisons of behavior of the natural peptides with that of their synthetic analogues. The decapeptides provide good models for iron(III) coordination by the parent protein. The biological and technological relevance of the iron(III)–DOPA interactions is discussed.

## Introduction

Mussels are known to accumulate high concentrations of metal ions from seawater. Many of these metals have been detected in their byssal threads at levels which often implicate these holdfasts as candidates for environmental markers of metal pollution.<sup>1–3</sup> Certain mytilid species display a degree of specificity for the type metal ion that is sequestered. Tateda and Koyanagi, for example, found that *Septifer virgatus* preferentially accumulated manganese from seawater while the common mussel *Mytilus edulis* sequestered higher concentrations of iron.<sup>4</sup> Iron is predominantly found in the adhesive plaques or disks (ca. 1700 μg/g of dry weight) but also in the threads (ca. 400 μg/g of dry weight) of *M. edulis* byssus.<sup>2</sup> Radioactive tracer studies employing iron-59 have shown that the metal accumulates in linear proportion to the seawater concentration, about 30% of that absorbed in the gut being ultimately excreted in the faeces, while 35% is transported by amoebocytes in the hemolymph from the gut to the byssus via the byssus gland complex.<sup>1</sup>

Polyphenolic proteins derived from a part of this complex, known as the phenol gland, and more recently from the byssal threads and plaques, have been intensively investigated.<sup>5–13</sup> A novel characteristic of many of these proteins is the presence

of 3,4-dihydroxyphenylalanine (DOPA) in their primary structure, produced by a post- or co-translational hydroxylation of tyrosine.<sup>5,11</sup> Waite<sup>5,6</sup> characterized peptides from tryptic digests of the first of these families of proteins, designated *M. edulis* foot protein 1 (Mefp1). His results suggested that Mefp1 consisted predominantly of tandemly repeated hexa- and decapeptide sequences with extensive hydroxylation of tyrosine to DOPA and also proline to 3- and 4-*trans*-hydroxyproline<sup>5,6</sup> (Figure 1). Filipula et al. and Laursen later confirmed this hypothesis by sequencing the appropriate genomic and cDNA's.<sup>12,13</sup>

The catecholic moiety of DOPA gives the proteins potent complexing power, the catechol siderophores forming some of the strongest complexes with iron(III) known.<sup>14</sup> The chelating potential of DOPA proteins may be important to processes of adhesion both by surface coupling with metals in marine substrata and by aiding in the process of quinone tanning to form an intractable, resistant matrix.<sup>15</sup>

In this paper we describe the complexation of iron(III) by both Mefp1 and its component peptides which have been isolated from tryptic digests of the parent protein as well as some synthetic decapeptide analogues. Since only submilligram quantities of these peptides were typically available, a sensitive

\* To whom correspondence should be addressed at the Department of Chemistry and Biochemistry. Fax: 302-831 6335.

<sup>⊗</sup> Abstract published in *Advance ACS Abstracts*, November 1, 1994.

- (1) George, S. G.; Pirie, B. J. S.; Coombs, T. L. *J. Exp. Mar. Biol. Ecol.* **1976**, *23*, 71.
- (2) Coombs, T. L.; Keller, P. J. *Aquat. Toxicol.* **1981**, *1*, 291.
- (3) Koide, M.; Lee, D. S.; Goldberg, E. D. *Est. Coast. Shelf Sci.* **1982**, *15*, 679.
- (4) Tateda, Y.; Koyanagi, T. *Bull. Jpn. Soc. Fish.* **1986**, *52*, 2019.
- (5) Waite, J. H. *J. Biol. Chem.* **1983**, *258*, 2911.
- (6) Waite, J. H.; Housley, T. J.; Tanzer, M. L. *Biochemistry* **1985**, *24*, 5010.
- (7) Pardo, J.; Gutierrez, E.; Sáez, C.; Brito, M.; Burzio, L. O. *Prot. Exp. Purif.* **1990**, *1*, 147.
- (8) Rzepecki, L. M.; Chin, S.-S.; Waite, J. H.; Lavin, M. F. *Mol. Mar. Biol. Biotech.* **1991**, *1*, 78.
- (9) Marumo, K.; Waite, J. H. *Biochim. Biophys. Acta* **1986**, *872*, 98.
- (10) Rzepecki, L. M.; Hansen, K. M.; Waite, J. H. *Biol. Bull.* **1992**, *183*, 123.
- (11) Benedict, C. V.; Waite, J. H. *J. Morphol.* **1986**, *189*, 171.
- (12) Filipula, D. R.; Lee, S.-M.; Link, R. P.; Strausberg, S. L.; Strausberg, R. L. *Biotechnol. Prog.* **1990**, *6*, 171.
- (13) Laursen, R. A. In *Results and Problems in Cell Differentiation*; Case, S. T., Ed.; Springer-Verlag: Berlin, 1992; Vol. 19, Chapter 3.
- (14) Raymond, K. N.; Müller, G.; Matzanke, B. F. In *Topics in Current Chemistry*; Boschke, F. L., Ed.; Springer-Verlag: Berlin, 1984; Vol. 123, pp 50–102.
- (15) Waite, J. H. *Comp. Biochem. Physiol.* **1990**, *97B*, 19.

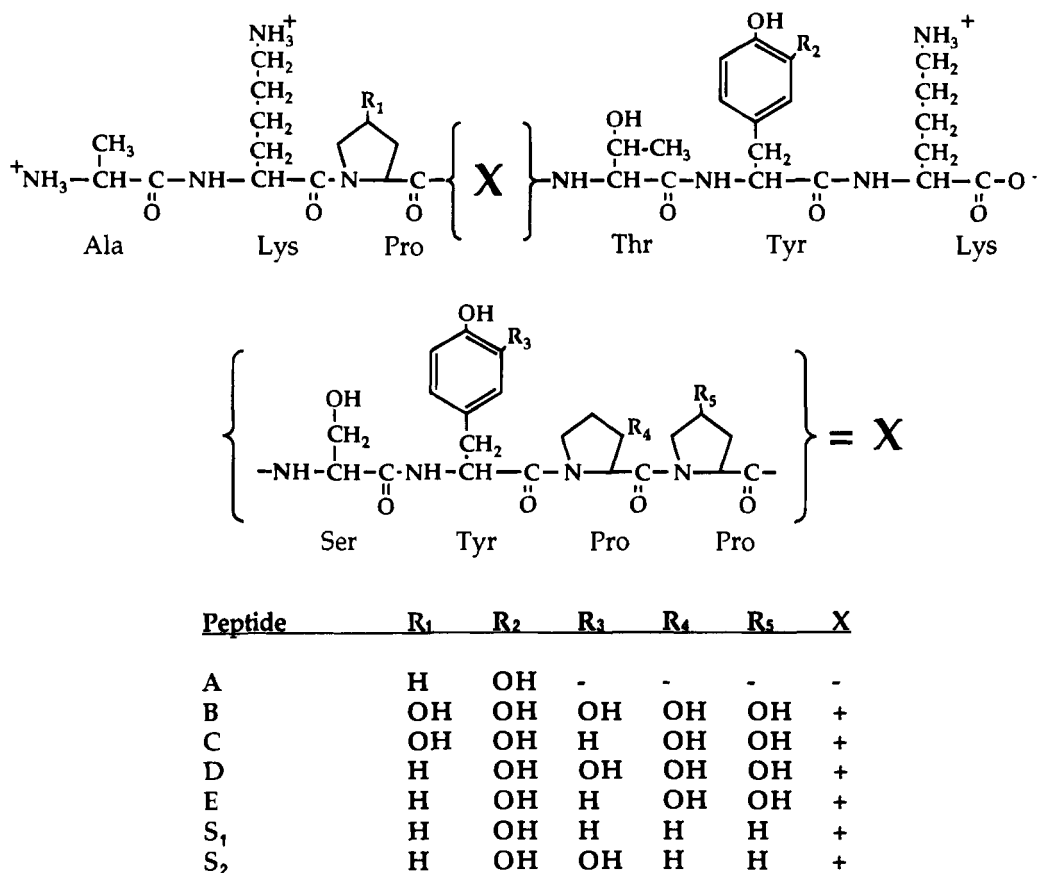


**Figure 1.** Structures of Mefp1 peptides A to E and synthetic peptides S<sub>1</sub> and S<sub>2</sub>.

measure of iron(III) complexation was in demand. Recently, a polarographic technique was developed that correlates the stability of a metal complex to its reduction potential.<sup>16</sup> By setting up a "chelate scale" with model complexes having known stability constants and readily measurable reduction potentials, it is possible to estimate the stability constants for the iron(III) peptide complexes at  $\mu$ molar concentrations. Spectroscopic evidence is also presented to give insights into the nature of the complexes formed by the peptides from a comparison with model complexes.

### Experimental Section

The isolation of Mefp1 and the tryptic peptides has been described previously.<sup>6,8</sup> Synthetic decapeptides were hydroxylated with mushroom tyrosinase as described by Marumo and Waite.<sup>9</sup> The purity of the protein was assessed by acid-urea electrophoresis and the peptides by amino acid and sequence analysis. Once purified, proteins were freeze dried and peptides flash evaporated then resuspended in distilled water prior to introduction to ferric ion. Proteins and peptides were quantified by the nitration assay for DOPA.<sup>17</sup> Enterobactin was a generous gift from Dr. E. McCafferty and was made up as a 1 mg/mL solution in methanol. All other ligands were obtained from Sigma and were made up as 10 mM stock solutions. Iron(III) solutions were prepared from a ferric chloride solution supplied as an atomic absorption standard from Sigma (1 mg/mL). Measurements were carried out in 5 mM bis(2-hydroxyethyl)iminotris(hydroxymethyl)methane (Bistris) buffer pH 7.0 at 25 °C with the ionic strength held constant at 0.1 M with NaCl. Ferric chloride was made up in 5 mL of this buffer and then titrated with ligand after sparging for 4 min with high purity argon.

Polarographic measurements were made with an EG&G Princeton Applied Research (PAR) Model 384B-4 polarographic analyzer with a model 303A mercury drop electrode and a saturated calomel reference

electrode (SCE). Analyses were performed in the square wave voltammetry (SWV) mode for increased sensitivity with a hanging mercury drop electrode. Further measurements were undertaken to assess the reversibility of the electrochemical processes according to the criteria outlined by Bond, performing experiments in the cyclic staircase voltammetry mode which will be abbreviated CV and measuring  $E_p$ 's with varying scan rate.<sup>18</sup> Electronic absorption spectra were recorded on a Cary 210 scanning spectrophotometer (Varian). Speciation calculations were performed using the thermodynamic equilibrium modeling program MINEQL<sup>19</sup> which were constrained to eliminate precipitation of  $\text{Fe}(\text{OH})_3$  to simulate the action of Bistris which stops hydrolysis by forming weak complexes with iron(III).<sup>20</sup> All log  $K$ 's are for  $I = 0.1$ , 25 °C, those from the literature being corrected using the equation<sup>19</sup>

$$\log K_i = \log K_0 - [z_M^2 + nz_L^2 - (z_M + nz_L)^2] \times [I^{1/2}/(I^{1/2} + 1) - 0.2I] \times 0.5 \quad (1)$$

for a complex  $\text{ML}_n$  where  $z_M$  and  $z_L$  are the ionic charges on the metal and ligand, respectively.

### Results and Discussion

**Chelate Scale.** For the reduction of a metal complex to one of lower valency with no change in metal–ligand stoichiometry, the half-wave potential,  $E_{1/2}$ , can be related to the stability

(16) Lewis, B. L.; Luther, G. W.; Lane, H.; Church, T. M. *Electroanalysis*, in press.

(17) Waite, J. H.; Tanzer, M. L. *Anal. Biochem.* **1981**, *111*, 131.

(18) Bond, A. M. *Modern Polarographic Methods in Analytical Chemistry*; Marcel Dekker, Inc.: New York, 1980; pp 195–196.

(19) Westall, J. C.; Zachary, J. L.; Morel, F. F. M. *MINEQL, a computer program for the calculation of chemical equilibrium composition of aqueous systems*, Technical Note 18, Department of Civil Engineering, MIT, 1976.

(20) Taylor, S. W. Ph.D. Thesis, The University of Queensland, Australia, 1993.

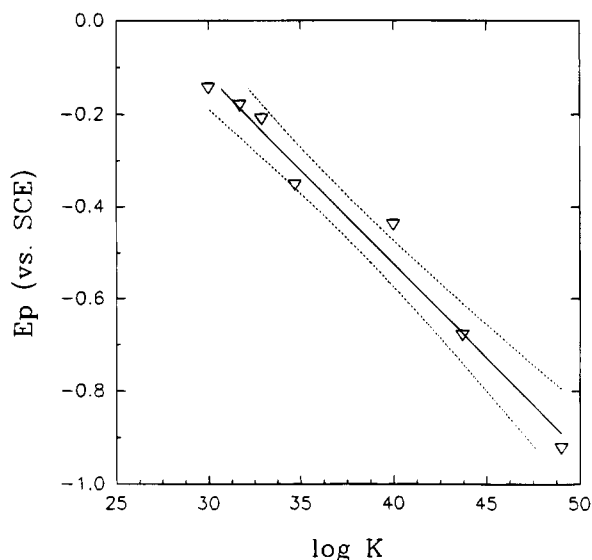


**Figure 2.** Chelate scale for iron(III) complexes listed in Table 1 ( $E_p = 1.104 - 0.041 \log K_{ox}$ ). Solid and dotted lines represent the linear regression through the data and the 95% confidence interval, respectively.

constants of the reduced and oxidized forms,  $K_{red}$  and  $K_{ox}$ , by the equation

$$E_{1/2}' = E_{1/2} - (2.303RT/nF) \log (K_{ox}/K_{red}) \quad (2)$$

where  $E_{1/2}$  is the reduction potential of the free metal ion and  $n$  is the number of electrons involved in the process.<sup>21</sup> This equation assumes that the electrode processes are reversible. In the current study, we chose conditions such that there is no change in metal–ligand stoichiometry on reduction of the complexes by titrating the metal with ligand until no further change in  $E_{1/2}'$  is observed. The reversibility of the electrode processes was checked as described in the Experimental Section. We have made use of this relationship by correlating the redox potentials of a series of iron(III) complexes with their known stability constants (Figure 2). For iron(III) in Bistris,  $E_{1/2}$  lies outside the window of the hanging mercury drop electrode; however, strong complexation brings the reduction potential of iron(III) to a readily observable voltage by increasing electron density around the metal center and making it more difficult to reduce. Since we are working with solutions containing only  $\mu\text{M}$  quantities of iron(III),  $E_p'$  is measured in SWV and CV experiments instead of  $E_{1/2}$ . However, as stated above, the reduction of a metal complex to one of lower valency,  $E_{1/2}'$  should be proportional to the ratio of the stability constants of the reduced and oxidized complexes<sup>21</sup> and not just that of the oxidized reactant. In the current investigation, an excellent correlation ( $r^2 = 0.98$ ) between the  $E_p$ 's obtained by SWV of the complexes and the log of their pH independent stability constants for the iron(III) complexes,  $K_{ox}$ , was observed. The reason for the  $K_{red}$  independence of  $E_{1/2}$  is unclear. Of our complexes, the only  $K_{red}$  constants known are for the ferrous complexes of CDTA,<sup>22a</sup> catechol<sup>22b</sup> and enterobactin.<sup>23,24</sup> The log  $K_{red}$  values for the enterobactin and CDTA complexes are identical and equal to 19, and the line of best fit through the

**Table 1.** Electrochemical and Stability Constant Data for Complexes in the "Chelate Scale"

complex <sup>a</sup>	$E_p$ (V) <sup>b,c</sup>	$\log K^d$ (25 °C, 0.1)	ref
[FeCDTA] <sup>-</sup>	-0.145	30.0	22a
[FeNTAiron] <sup>4-</sup>	-0.182	31.7	27
[FeNTAcac] <sup>2-</sup>	-0.211	32.9	28
[Fe(cat) <sub>2</sub> ] <sup>-</sup>	-0.354 <sup>e</sup>	34.7	29
[Fe(4Ncat) <sub>3</sub> ] <sup>3-</sup>	-0.440 <sup>e</sup>	40.0	29
[Fe(cat) <sub>3</sub> ] <sup>3-</sup>	-0.680 <sup>e,f</sup>	43.7	29
[Fe(ent)] <sup>3-</sup>	-0.924	49.0	23

<sup>a</sup> CDTA = *cis*-1,2-cyclohexylenedinitrilotetraacetate, NTA = nitrilotriacetate, iron = 4,5-dihydroxy-1,3-benzenedisulfonic acid, cat = catechol, 4Ncat = 4-nitrocatechol, ent = enterobactin. <sup>b</sup> 5 mM Bistris pH 7.0, 0.1 M NaCl (20  $\mu\text{M}$  iron(III)). <sup>c</sup>  $\pm 10$  mV. <sup>d</sup> Adjusted to ionic strength,  $I = 0.1$ , if necessary, using eq 1. <sup>e</sup> 10  $\mu\text{M}$  iron(III). <sup>f</sup> pH 10.0.

three complexes is parallel to the  $\log K_{ox}$  versus  $E_p$  plot although the regression is substantially poorer ( $r^2 = 0.90$ ). This is due to the behavior of the bis(catecholato) complex which is known to have a more complicated chemistry than the other complexes, for example, by forming binuclear catecholate bridged species.<sup>25</sup> If, with the exception of this complex, the  $K_{red}$  values for all our complexes are similar, then the  $K_{red}$  term could be incorporated into the intercept

$$E_{1/2}' = [E_{1/2} + (2.303RT/nF) \log K_{red}] - (2.303 RT/nF) \log K_{ox} \quad (3)$$

resulting in a highly significant correlation for the  $\log K_{ox}$  versus  $E_p$  plot. The slope of this plot should be 0.059 for a single electron reduction. We obtained a value of 0.041. The lesser slope may be accounted for by variance in  $K_{red}$ 's for the different complexes. The enterobactin and CDTA iron complexes'  $K_{red}$  values aside, an undetermined proportionality between  $\log K_{ox}$  and  $\log K_{red}$  may exist for the complexes in the series. This would also result in a linear plot with a slope different to the Nernst value. Adjustment of reported stability constants to conditional constants is unnecessary because the correction for deprotonation of the ligands at a given pH will be identical for both  $K_{ox}$  and  $K_{red}$ .

This "chelate scale" may be used for an empirical estimation of  $K$  for an unknown. This method was first adopted by Hoyle and West to estimate the stability constants of some "complex-one" type ligands with copper(II)<sup>26</sup> and values obtained for some unknowns were in close agreement with later estimates.<sup>22</sup> More recently, Lewis and co-workers applied the method in studying zinc complexation by organic material in natural waters.<sup>16</sup>

Seven ferric complexes spanning 20 orders of magnitude of chelate stability make up our chelate scale. Polarographic and stability constant data are summarized in Table 1. The catecholate ligands are likely to provide good models for iron(III) chelation by the DOPA-containing peptides and proteins. Despite the fact that the complexes were of varying stoichiometries, had mixed and nonmixed coordinating ligands and redox inactive and active ligands it can be clearly seen from Figure 2 that a linear relationship between  $E_p'$  and  $\log K$  was observed.

Speciation calculations show that [FeCDTA]<sup>-</sup>, [FeNTAiron]<sup>4-</sup>, [FeNTAcac]<sup>2-</sup>, [Fe(cat)<sub>2</sub>]<sup>-</sup>, [Fe(cat)<sub>3</sub>]<sup>3-</sup> and [Fe(ent)]<sup>3-</sup> were the predominant species in their respective solutions, a fact confirmed by spectral data for the last five complexes which had visible maxima at 570 nm ([FeNTAiron]<sup>4-</sup>), 610 and 408 nm ([FeNTAcac]<sup>2-</sup>), 570 ([Fe(cat)<sub>2</sub>]<sup>-</sup>), 480 nm ([Fe(cat)<sub>3</sub>]<sup>3-</sup>), and

(21) Heyrovský, J.; Kůta, J. *Principles of Polarography*; Academic Press: New York, 1966; pp 156–158.

(22) Smith, R. M.; Martell, A. E. *Critical Stability Constants*; Plenum Press: New York: (a) Vol. 1, 1977, pp 236; (b) Vol. 3, 1977, pp 200; (c) Vol. 6, 1989, pp 435.

(23) Loomis, L. D.; Raymond, K. N. *Inorg. Chem.* **1991**, *30*, 906.

(24) Lee, C.-W.; Ecker, D. J.; Raymond, K. N. *J. Am. Chem. Soc.* **1985**, *107*, 6920.

(25) Gahan, L. R.; Grillo, V. A.; Hambley, T. W.; Hanson, G. R.; Murray, K. S. Unpublished results.

(26) Hoyle, W.; West, T. S. *Talanta* **1959**, *2*, 158.

490 nm ( $[\text{Fe}(\text{ent})]^{3-}$ ) in agreement with data reported in the literature.<sup>23,27-29</sup> In the case of  $[\text{Fe}(\text{4Ncat})_3]^{3-}$  it was necessary to use an excess of metal over ligand so that the complex peak at  $-0.440$  V could be resolved from a prominent 4Ncat reduction peak at  $-0.568$  V. The visible spectrum displayed a shoulder at 490 nm characteristic of the tris-chelated species on the 410 nm absorption band due to the ligand confirming the presence of the complex. As the ligand concentration was increased to 1:1 ligand:metal (at which point the tris(4-nitrocatecholato)ferrate(III) is formed exclusively at pH 7.0<sup>29</sup>), the complex peak became a shoulder on the ligand reduction peak but without changing potential, thus establishing the ligand concentration independence of  $E_{1/2}$  which is important in application of eq 2.

All polarograms contained either a single symmetric peak attributable to the designated complex or additional peaks attributable to reduction of excess free ligand as gauged by parallel measurements on the ligand added to Bistris buffer alone (Figure 3). Most noticeable in the latter case was a peak at  $-0.568$  V in the reduction of 4Ncat (as discussed above), a peak at  $-0.15$  V in the pH 10.0 solution of tris(catecholato)ferrate(III) possibly due to reduction of free semiquinone to catechol and a peak at  $-1.20$  V in ferric enterobactin solutions. Iron(II) reduction peaks were also observed around  $-1.4$  to  $-1.5$  V for each species.

The reversibility of electrode processes for each of the complexes was investigated by examining the appearance of the CV's and their behavior with varying scan rate. It was demonstrated that the  $[\text{FeCDTA}]^-$  and  $[\text{Fe}(\text{ent})]^{3-}$  reductions were unequivocally reversible,  $E_p$ 's not shifting when the scan rate was increased from 10 to 100  $\text{mV s}^{-1}$ . The  $[\text{Fe}(\text{4Ncat})_3]^{3-}$  peak was obscured by the irreversible ligand reduction peak in the CV and could not be observed. Other complexes'  $E_p$ 's moved from 10 to 20 mV more negative with increasing scan rate, with the exception of  $[\text{Fe}(\text{cat})_2]^-$  which showed a larger 56 mV shift to more negative potentials. While these shifts may be indicative of irreversible electrode processes, they are also consistent with processes that are quasi-reversible with adsorption. Adsorption of catechol-like ligands apparently occurs as a result of the interaction of  $\pi$ -orbital electrons with the mercury drop which increases sensitivity and gives these ligands utility in electrochemically determining trace amounts of ferric ion.<sup>30,31</sup> This is confirmed by the presence of nonzero anodic currents in the CV's of each of the complexes, albeit small and broad in the case of bis(catecholato)ferrate(III) (Figure 3d).

The chelate scale based on these complexes presented in Figure 2 is for a 20  $\mu\text{M}$  concentration of ferric iron (with the exception of the bis- and tris(catecholato)ferrate(III) and tris(4-nitrocatecholato)ferrate(III) which were measured at 10  $\mu\text{M}$  because of the presence of an additional peak at higher concentrations (possibly attributable to bridged binuclear iron(III) complexes as isolated by Gahan et al.<sup>25</sup>). Almost identical results were obtained at 3  $\mu\text{M}$  iron(III) for the strongly adsorbed ferric complexes (the  $[\text{FeCDTA}]^-$  reduction peak was not observed at the lower concentration). This is important as the lower concentration was employed for our peptide measurements. The plot is linear ( $r^2 = 0.98$ ) although  $n$  is nonintegral

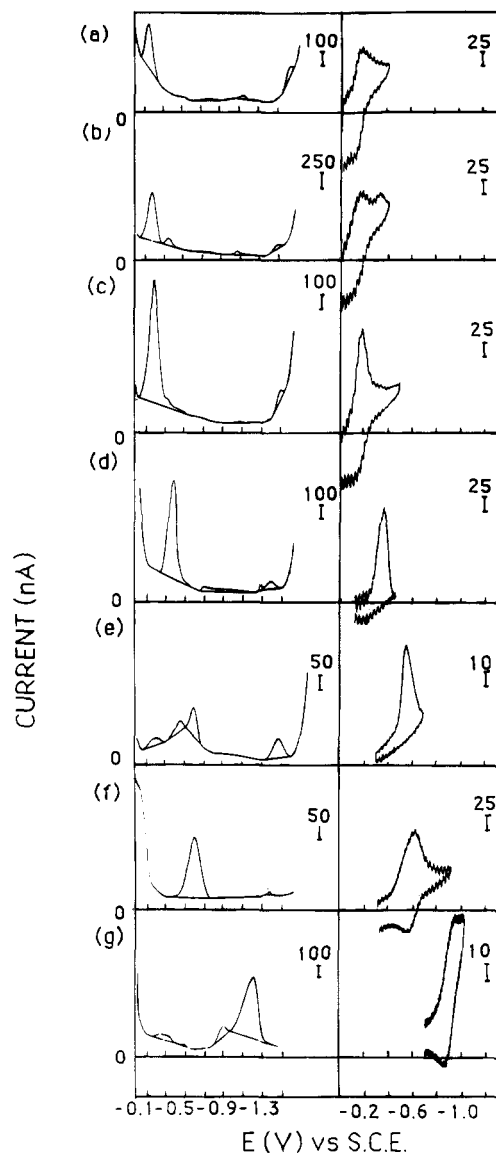


**Figure 3.** SWV and CV polarograms: (a)  $[\text{FeCDTA}]^-$  ( $[\text{Fe}]_{\text{T}} = 20 \mu\text{M}$ ,  $[\text{CDTA}]_{\text{T}} = 30 \mu\text{M}$ ); (b)  $[\text{FeNTA}(\text{iron})]^{4+}$  ( $[\text{Fe}]_{\text{T}} = 20 \mu\text{M}$ ,  $[\text{NTA}]_{\text{T}} = 900 \mu\text{M}$ ,  $[\text{tiron}]_{\text{T}} = 10 \mu\text{M}$ ); (c)  $[\text{FeNTAcac}]^{2-}$  ( $[\text{Fe}]_{\text{T}} = 20 \mu\text{M}$ ,  $[\text{NTA}]_{\text{T}} = 900 \mu\text{M}$ ,  $[\text{cat}]_{\text{T}} = 40 \mu\text{M}$ ); (d)  $[\text{Fe}(\text{cat})_2]^-$  ( $[\text{Fe}]_{\text{T}} = 10 \mu\text{M}$ ,  $[\text{cat}]_{\text{T}} = 40 \mu\text{M}$ ); (e)  $[\text{Fe}(\text{4Ncat})_3]^{3-}$  ( $[\text{Fe}]_{\text{T}} = 10 \mu\text{M}$ ,  $[\text{4Ncat}]_{\text{T}} = 2 \mu\text{M}$ ); (f)  $[\text{Fe}(\text{cat})_3]^{3-}$  ( $[\text{Fe}]_{\text{T}} = 10 \mu\text{M}$ ,  $[\text{cat}]_{\text{T}} = 50 \mu\text{M}$ ); (g)  $[\text{Fe}(\text{ent})]^{3-}$  ( $[\text{Fe}]_{\text{T}} = 20 \mu\text{M}$ ,  $[\text{ent}]_{\text{T}} = 20 \mu\text{M}$ ). Conditions: scan rate, 200  $\text{mV s}^{-1}$  (SWV), 100  $\text{mV s}^{-1}$  (CV); pulse height, 20 mV; frequency, 100 Hz. Scale bars are in nA.

(see above) and the intercept reflects a value for the  $E_p$  of ferric ion weakly complexed by Bistris as well as a contribution from  $0.041 \log K_{\text{red}}$ , which, assuming  $\log K_{\text{red}}$  for all complexes equals 19, gives a value of 0.324 V for the  $E_p$  of FeBistris.

**Ferric Enterobactin.** The electrochemistry of ferric enterobactin complexes has been studied extensively by Raymond and co-workers.<sup>24,32,33</sup> The earlier studies described a pH dependent iron(III) complex reduction peak which became increasingly irreversible below pH 10.<sup>32,33</sup> This was later found to be a consequence of the incorporation of borate as a buffer<sup>24</sup> which forms complexes with both catechols<sup>34</sup> and iron(III).<sup>22c</sup> The

(27) Morin, M.; Scharff, J. P. *Anal. Chim. Acta* **1973**, *66*, 113.

(28) Taylor, S. W.; Hawkins, C. J.; Winzor, D. J. *Inorg. Chem.* **1993**, *32*, 422.

(29) Avdeef, A.; Sofen, S. R.; Bregante, T. L.; Raymond, K. N. *J. Am. Chem. Soc.* **1978**, *100*, 5362.

(30) van den Berg, C. M. G.; Huang, Z. Q. *J. Electroanal. Chem.* **1984**, *177*, 269.

(31) van den Berg, C. M. G. *Analyst* **1989**, *114*, 1527.

(32) Cooper, S. R.; McArdle, J. V.; Raymond, K. N. *Proc. Natl. Acad. Sci. U.S.A.* **1978**, *75*, 3551.

(33) Harris, W. R.; Carrano, C. J.; Cooper, S. R.; Sofen, S. R.; Avdeef, A. E.; McArdle, J. V.; Raymond, K. N. *J. Am. Chem. Soc.* **1979**, *101*, 6097.

(34) Waite, J. H. *Anal. Chem.* **1984**, *56*, 1935.

**Table 2.** Polarographic and Spectrophotometric Data for Mefp1 Peptides A to E

peptide (concn, ( $\mu\text{M}$ ))	$E_p$ (V) <sup>a,b</sup> (i (nA))	abs max (nm) ( $\epsilon$ ( $\text{M}^{-1} \text{cm}^{-1}$ ))	$\log K_{\text{est}}^c$ (25 °C, 0.1)
A (34.6)	-0.456 (129)	570 (1423)	38.0
B (11.7)	-0.532 (205)	570 (2580)	39.9
C (16.5)	-0.522 (182)	570 (2430)	39.7
D (17.5)	-0.518 (160)	570 (3125)	39.6
E (15.0)	-0.516 (144)	570 (2080)	39.5
S <sub>1</sub> (38.5)	-0.488 (98)	570 (1570)	38.8
S <sub>2</sub> (20.0)	-0.506 (156)	570 (2780)	39.3
Mefp1 (0.5)	-0.542 (41) <sup>d</sup> ~-0.60 (sh)	515 (2000)	40.1 ~41.6

<sup>a</sup>  $\pm 10$  mV. <sup>b</sup> 5 mM Bistris pH 7.0, 0.1 M NaCl (3  $\mu\text{M}$  iron(III)).  
<sup>c</sup>  $\pm 1$  to 1.5 log units. <sup>d</sup> 18.5  $\mu\text{M}$  iron(III).

pH dependence was ascribed to protonation of the catechol moieties in the ferrous complexes and was used to determine the ferrous enterobactin stability constant.<sup>24</sup> In the absence of borate (20 mM phosphate buffer pH 7.0, 2 M  $\text{NH}_4\text{Cl}$ ) a reversible reduction was observed at pH 7.4 at -1.03 V (vs SCE) in good agreement with the peak at -0.924 V observed in the current investigation at pH 7.0. We also found at lower [Fe]:[ent] ratios two peaks were observed around -0.52 to -0.56 V and -0.75 to -0.78 V while the visible absorption spectra were identical with a maximum at 490 nm. These peaks may reflect intermolecular tris(catecholato) coordination of iron(III) by two or more enterobactin molecules. Having the catechols coming from different molecules would be less energetically advantageous because there would be less entropy.

**Mefp1 Peptides A to E.** The predominant repeating amino acid sequences of Mefp1 are readily isolated as peptides from tryptic digests of Mefp1.<sup>5,6</sup> Peptide A was the only hexapeptide isolated in sufficient quantities for the studies described herein, while decapeptides B to E differ only in their degree of hydroxylation, either of proline-3 and/or tyrosine-5 to 4HYP-3 and/or DOPA-5, respectively (Figure 1).<sup>5,6</sup> Each peptide should readily coordinate iron(III) through DOPA-9; however only peptides B and D can form totally intramolecular bis(catecholato)iron(III) complexes. Any coordination mode involving more than one catechol in peptides A, C and E, and more than two catechols in D and E, clearly must be intermolecular. Fortunately, the spectral characteristics of iron(III) catechol complexes have been well documented, mono(catecholato) coordination having an absorption maximum at greater than 650 nm, bis(catecholato) at 570 nm, and tris(catecholato) at 490 nm.<sup>29</sup> By correlating polarographic data for the peptides to stability constants using the chelate scale described above, and spectrophotometric data to spectral data for known model compounds, it is possible to compare and contrast the various iron(III) complexes formed by the different peptides.

Results of polarographic and spectrophotometric data for the iron(III) peptide complexes are summarized in Table 2. Representative visible spectra and polarograms are illustrated in Figures 4 and 5. All peptides formed bis(catecholato)iron(III) complexes as gauged by the visible absorption maximum at 570 nm. Clearly, this demonstrates that peptides A, C and E are forming intermolecular peptide complexes. The possibility of intramolecular bis(catecholato) coordination of iron(III) by peptides B and D is unlikely given that the reduction potentials for all peptides were similar to peptides C and E (around -0.52 V). For entropy reasons, intramolecular coordination by two DOPA residues should confer greater stability and hence a more negative  $E_p$  as discussed above for enterobactin.  $E_p$ 's shifted -68, -42, -38, -48 and -22 mV when the scan rate was increased from 10 to 100  $\text{mV s}^{-1}$  for peptides A to E, respectively; however, CV scans of all the above peptide

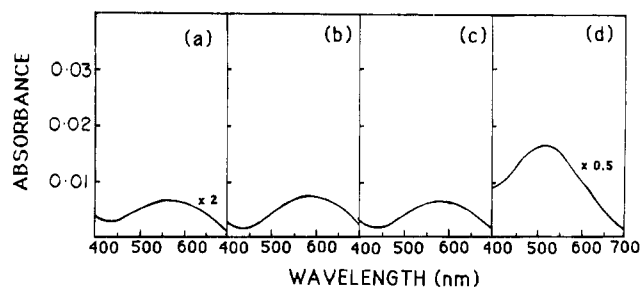


**Figure 4.** Typical visible spectra of iron(III) in Bistris in the presence of Mefp1 peptides: (a) peptide A; (b) peptide B; (c) peptide C; (d) Mefp1 ([Fe]<sub>T</sub> = 2.9  $\mu\text{M}$  for each of the peptides, [peptide A]<sub>T</sub> = 34.6  $\mu\text{M}$ , [peptide B]<sub>T</sub> = 11.7  $\mu\text{M}$ , [peptide C]<sub>T</sub> = 16.5  $\mu\text{M}$ ; [Fe]<sub>T</sub> = 18.5  $\mu\text{M}$  for the protein, [Mefp1]<sub>T</sub> = 0.5  $\mu\text{M}$ ).

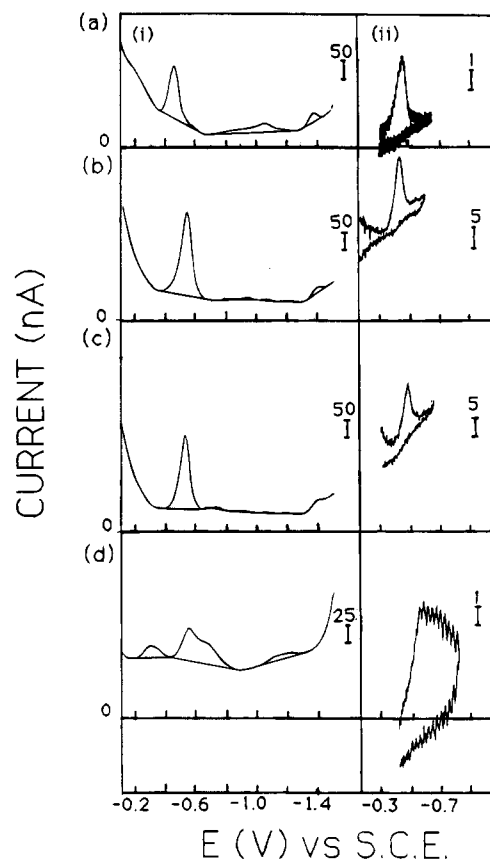


**Figure 5.** Typical polarograms corresponding to the spectra in Figure 4 of iron(III) in Bistris in the presence of Mefp1 and its component peptides (i) SWV and (ii) CV: (a) peptide A; (b) peptide B; (c) peptide C; (d) Mefp1. Conditions are in Figure 2 but with scan rate 10  $\text{mV s}^{-1}$  for the CV's in (b) and (c).

complexes displayed very small, broad but nonzero anodic currents (more apparent at the slower scan rate) which is indicative of adsorption.<sup>18</sup>

All the bis(catecholato) coordinated species have  $E_p$ 's considerably more negative than the simple catechol-iron(III) complexes, while  $E_p$ 's in SWV's of the decapeptide complexes appear at slightly more negative potentials than those of the hexapeptide. Because of adsorption, the dependence of  $E_p$  on scan rate discussed above means that the stability constants calculated from Figure 2 may be overestimates by 0.5 to 1.7 log units. The remaining discrepancies between the peak potentials of the simple catechol complexes and the hexa- and decapeptide complexes can be accounted for by extra stability in the latter. Since there is no entropy advantage if the DOPA's come from different peptide molecules, then the involvement of one or more other groups in binding iron(III) is implied. The carboxyl

termini can be eliminated because steric restrictions preclude them from coordinating in conjunction with DOPA-9. This leaves the hydroxyproline, serine and threonine residues as the only other potential coordinating side chains. However, the  $pK_a$ 's of the hydroxyl side chains of these residues (in simple peptides) will be too high to make them likely contenders for metal coordination. Perhaps hydrogen bonding to a coordinated water could also explain the enhanced stabilization in peptide-iron(III) complexes containing these residues. Molecular models suggest that the threonine adjacent to DOPA-5 in peptide A and DOPA-9 in peptides B to E,  $S_1$  and  $S_2$  could potentially fulfill this role. To test whether there is any involvement of the hydroxyproline residues of the decapeptides in binding iron(III), a synthetic peptide analogue of the natural decapeptides, containing no hydroxyprolines and tyrosine in the 5 and 9 positions, was enzymatically hydroxylated with mushroom tyrosinase to form DOPA peptides. Before hydroxylation, the peptide did not bind iron(III) as gauged by the absence of peaks in the polarogram and lack of absorbance in the visible region. After hydroxylation of the tyrosine to DOPA residues (in the 9 position for  $S_1$  and 9 and 5 positions for  $S_2$ ), iron binding was directly analogous to that of the natural peptides B to E. This points against hydroxyproline involvement in iron(III) coordination. The only amino acid present in peptides B to E and not present in peptide A that may account for the enhanced stability in the former peptide complexes is serine-4. Hydrogen bonding by this residue to a coordinated water may produce a more energetically favorable structure. Unfortunately these hypotheses are not readily checked by further experimentation with only submilligram quantities of peptides available.

**Mefp1.** Mefp1 proved more difficult to handle than the component peptides. At neutral to alkaline pH values, the protein tends to precipitate. In addition, Mefp1 was found to stick to the platinum counter electrode and glassware. Despite these problems, good spectra and SWV polarograms were obtained by titrating 20  $\mu$ M iron(III) in Bistris buffer with the protein (Figures 4(d) and 5(d)), although the broad CV made it difficult to judge the reversibility of the electrode processes. The SWV polarographic peak developed at  $-0.458$  V and shifted to  $-0.542$  with a shoulder at  $\sim -0.6$  V with excess DOPA ( $[Mefp1] = 0.5 \mu$ M,  $[DOPA] = 75.0 \mu$ M). The corresponding visible spectrum showed a maximum at 515 nm. These data would suggest that the peptide complexes closely approximated coordination by the protein, although the protein tends to have a mixture of tris- and bis(catecholato) coordination

environments as indicated by the shoulder at  $-0.6$  V (closer to the  $E_p$  of tris(catecholato)ferrate(III)) and the visible maximum being intermediate between that for bis- and tris-chelated iron(III) complexes.

## Conclusions

The following conclusions pertain to the interactions of iron(III) with the proteins and peptides described in this paper:

(1) Spectrophotometric data suggest intermolecular coordination of iron(III) by peptides A, C and E as they only have 1 DOPA per peptide molecule yet initially have maxima at 570 nm indicative of bis(catecholato)iron(III) coordination.

(2) Since peptides B and D have iron(III) binding strengths similar to those of C and E, they too may be forming intermolecular complexes implicating DOPA-9 as the chelating residue.

(3) All bis(catecholato) peptide complexes have log  $K$ 's greater than the simple complex, and appear to involve intermolecular coordination. The extra stability may be conferred by hydrogen bonding interactions of serine and threonine residues to a coordinated water, however, studies on synthetic peptides point against the hydroxyproline residues at positions 6 and 7 playing a role in iron binding.

(4) The decapeptides provide good models for iron(III) coordination by the parent protein.

The excretion of high concentrations of iron into the byssus by *M. edulis* may serve a dual purpose. As well as ridding the organism of a potentially toxic iron overload, the metal may provide a functional advantage by acting as a cross-linker of proteins in the byssus threads. Such a role has been proposed previously for the DOPA-protein ferreascidin from the stolidobranch ascidian *Pyura stolonifera*<sup>28</sup> and for Mefp1 from *M. edulis*<sup>15</sup> although the current study represents the first report of iron binding in solution of the latter protein. Hansen has measured the adsorptive properties of Mefp1 with regard to steel and has found that the protein acts as an effective inhibitor of corrosion.<sup>35</sup> Studies such as those described herein may prove useful in assessing the affinity of the protein for various surface metals.

**Acknowledgment.** This research was supported by the ONR MIMI Program and an NIH Restorative Materials grant (J.H.W.) as well as NSF Grant OCE-9313020 (G.W.L.).

(35) Hansen, D. C. Ph.D. Thesis, University of Delaware, 1993.